Optimization of CESR-c Optics for High Time-Integrated Luminosity

M. Van Camp
Lawrence University, Appleton, WI, 54911
(Dated: 11 August, 2007)

The Cornell Electron Storage Ring (CESR) is known for its world-record time-integrated luminosity for studies of charm quark bound states produced in e^-/e^+ interactions. A new program, *dynap_scan*, was created to examine the effects of positron bunch current and e^+/e^- orbit on dynamic aperture at the interaction point in CESR-c, a factor known to limit lifetime. This program was used to find the combination of current and pretzel amplitude that maximized dynamic aperture width in the lattice 3007_inj_20070606_2p0_mult, with the goal of maximizing time-integrated luminosity. The likelihood of achieving high time-integrated luminosity from the parameters suggested by *dynap_scan* was tested by examining the Welch/Temnykh B parameter, horizontal beam-beam interaction kicks, and 500-turn phase space at the interaction produced by these settings. *Dynap_scan* successfully found a positron current and prz1 amplitude that is likely to increase time-integrated luminosity, making *dynap_scan* a useful new tool in lattice design and tuning.

I. Introduction

The Cornell Electron Storage Ring (CESR) is known both for its world-record production of charmonium, and for its use of pretzel orbits to control the collision of counterrotating electron and positron beams within the ring. A limiting factor in maintaining CESR's high luminosity is the management of the beam-beam interaction (BBI), both at the interaction point (IP) and at the parasitic crossings, which are locations in the pretzel orbits where electron and positron bunches pass each other. Two important parameters in managing BBI are the amplitude of the pretzel orbits and the current in the beams. By modifying one of Cornell's existing Fortran simulations of CESR, a new program, *dynap_scan*, was created to find the optimal combination of these parameters with respect to the dynamic aperture at the interaction point. The results of this program were then verified by examining the Welch/Temnykh B parameter and BBI kicks throughout the ring, as well as the 500-turn phase space at the IP. *Dynap_scan* has practical implications in the design of new lattices since it can suggest candidates for initial pretzel and current settings, thus reducing the time required to tune the lattice.

II. Storage Ring Optics

The electrons used in CESR are produced by a D.C. electron gun, which boils them off of a metal filament. The electrons are separated into discrete bunches, then accelerated to 300MeV in the linear accelerator. The beam is then further accelerated to the desired final energy in the synchrotron[1] and injected into CESR. Positron beams are produced by directing electrons in the linac into a tungsten plate. The impact produces photons, electrons, and positrons. The positrons are magnetically separated from the other particles, bunched, and accelerated like the electron beam. They are then injected into CESR such that they orbit in the opposite direction as the electrons. Since the electron and positron beams are not produced simultaneously, CESR's role is to store and manipulate the counterrotating beams in such a way as to maximize the number of collisions occurring in the CLEO detector. As the beams decay, additional electrons and positrons are injected to "top off" the beams and maintain efficient charmonium production. When CESR is being used for CLEO physics, it is commonly referred to as CESR-c.

A. CESR-c Lattice Components

1. Dipole Magnets

There are two primary challenges to storing a beam of charged particles: controlling its trajectory, and compensating for Coulombic repulsion within

[1] Cornell's synchrotron is capable of producing 5GeV beams, but it is currently operating at 1.8GeV to study charm quark bound states.

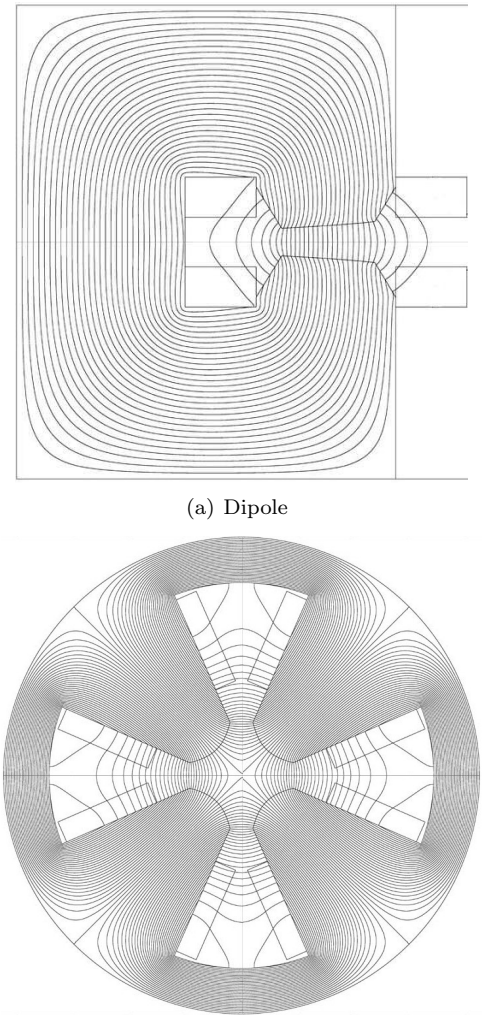

(a) Dipole

(b) Quadrupole

Figure 1: Guide magnet field lines.

the beam. To bend the beams' trajectories through the storage ring, a force is required perpendicular to the velocity of the beams. By the Lorentz force law,

$$\vec{F_L} = q(\vec{E} + \vec{v} \times \vec{B}), \tag{1}$$

it is clear that this can easily be done by placing the beams in a magnetic field perpendicular to their velocity.[1] This is accomplished with a series of dipole electromagnets, each oriented to produce a region of near-constant magnetic field proportional to the applied current:

$$\vec{B_{dip}} = \frac{2\mu_o NI}{h}. \text{ [1]} \tag{2}$$

Since the electron and positron beams are both oppositely charged and traveling in opposite directions, they are respond identically to the dipoles and can thus be managed with a single set of magnets.

Dipole-based rings, however, are very vulnerable to vertical perturbations in the beam since, as Eq. 1 shows, in a constant field perpendicular to the particle's path, perturbations parallel to the field introduce a vertical component to the force that will result in the particle spiraling out of the pipe. Early synchrotrons made use of *weak focusing*, an effect caused by introducing a field gradient in the dipoles to provide a vertical restoring force, but the energies accessible by such accelerators were limited by the need for large horizontal apertures to contain the orbit displacements caused by small angular deflections from the design orbit. Horizontal dispersion of the beam is inevitable in dipole-dominated rings, since no force is applied to counteract the horizontal component of the Coulomb force between particles of like charge within a beam[1]:

$$F_C = \frac{1}{4\pi\varepsilon_o}\frac{q^2}{r^2}. \tag{3}$$

This effect is reduced by the relativistic velocity of the beam, but if left unchecked this repulsion eventually disperses the beam beyond the limits of the beam pipe, thus reducing the current to unusable levels.

2. Quadrupole Magnets

It was not until the development of *strong focusing* by Courant, Livingston, and Snyder in 1952 that high-energy regimes became accessible[2]. Strong focusing works by utilizing quadrupole magnets of different orientations to focus the beams. The effect of a quadrupole magnetic field on a beam of charged particles is much like the effect of a thin glass lens on a beam of light, with the exception that a quadrupole can only focus in one transverse plane at a time. As suggested by the field lines in Fig. 1(b), there is a region in the center of a quadrupole where the field strength increases linearly with distance from the center of the magnet. In this region, in one plane a particle of a given charge will experience a restoring force toward the symmetry axis of the magnet and this force will increase linearly with the particle's displacement from the center. In the other plane, the same particle will experience a similar force pushing it away from the center line. This results in an incoming beam of particles being focused in one plane at a fixed focal length. Net focusing in both planes, however, can be achieved through what is known as a FODO (focusing/defocusing) lattice, a combination of focusing and defocusing quadrupoles separated by a

carefully chosen drift space. Assuming that the horizontally and vertically focusing quadrupoles have the same focal length, a net focusing in both planes can be achieved at a focal length f_{net} by separating the quadrupoles by a distance d such that d is less than twice the quadrupole focal length[3]:

$$\frac{1}{f_{net}} = \frac{2f_{quad} - d}{f_{quad}^2}. \quad (4)$$

By manipulating d the focal length of a two-quadrupole system can be adjusted over a wide range, allowing the beam to be focused to suit the needs of the accelerator or storage ring. The focusing and defocusing of a beam around the ring is described by its *betatron oscillation* (Fig. 2), the transverse oscillations of particles in the beam about the design orbit. The number of oscillations per orbit is referred to as the *tune*. The tune increases with focus, since finely focused beams have smaller oscillations away from the design orbit. The horizontal tune in CESR is slightly above 10.5, and the vertical tune is near 9.5. It is important, however to avoid integer, half-integer, and even rational tunes since they produce *resonances*. When a particle hits a resonant tune, every time it passes a given element of the lattice it does so at the same point in its betatron oscillation. The particle thus experiences a force pushing it in the same direction each time it passes that element, ultimately causing the particle to stray so far that it leaves the beam pipe.

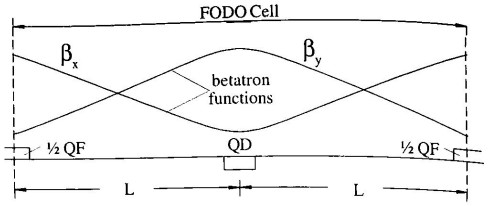

Figure 2: A FODO lattice element demonstrating betatron oscillation in x and y. [3]

3. Electrostatic Separators

If the counterrotating electron and positron beams were allowed to travel along the same orbit, they would collide at every location where two trains crossed paths. To prevent this, the beams are pulled into *pretzel orbits* (Fig. 3) by electrostatic separators. The separators provide a region of constant potential, which pulls the electron and positron beams toward the opposite poles of the separators by electrostatic attraction. There are not individual separators for each crossing; rather, four separators are used in concert to set up a standing oscillation about the center of the beam pipe. This is possible because of the betatron oscillation–each separator provides a horizontal 'kick' to the *entire* beam (as opposed to a single particle) causing the beam as a whole to develop an oscillation proportional to the betatron tune. The regions of maximum separation between the electron and positron orbits are known as *parasitic crossings* since, despite the separation, the beams still interact electromagnetically as the bunches pass each other.

B. Beam-Beam Interaction

In addition to the intended focusing and defocusing from the quadrupoles, interactions between the electron and positron beams provide additional focusing and defocusing. There are two types of this *beam-beam interaction*: the primary interaction at the interaction point, and interactions at the parasitic crossings. Interaction point beam-beam interaction (IPBBI) results in a horizontal and vertical focusing of the colliding beams due to Coulombic attraction between the electrons and positrons. This can cause significant shifts in the horizontal and vertical tunes, so it is vital to ensure that the beams are in collision when analyzing beam behavior under high-energy physics conditions. One cannot assume that a lattice will automatically collide the beams under its default parameters, however, since the primary goal of lattice design is minimizing beam size

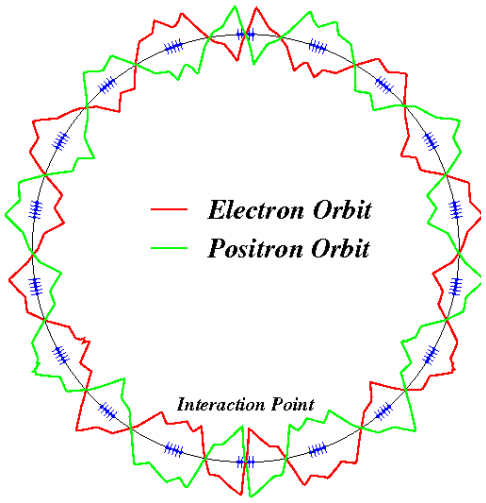

Figure 3: Pretzel orbits in CESR-c. The blue hash marks indicate the location of parasitic crossings.

at the IP, not necessarily finding parameters that optimize collision. It is thus important to find and implement separator and quadrupole settings that provide good beam collision.

Long-range beam-beam interaction (LRBBI) is caused by repulsion (due to relativistic effects) between the electron and positron beams as they pass each other at the parasitic crossings. The parasitic crossings thus act like additional defocusing quadrupoles in the lattice and cause the horizontal tune to decrease. The BBI-induced tune shifts cause the beams to encounter lattice elements at different points in their betatron oscillation than was intended in the lattice design, resulting in altered performance of the lattice and increasing the risk of hitting a resonant tune.[4][5][6]

C. Time-Integrated Luminosity

Luminosity is the instantaneous rate of collision per unit cross section, and is given by

$$\mathcal{L} = \frac{N_{e^-} N_{e^+}}{BA} f_{rev} \qquad \left[\frac{1}{cm^2 s}\right] \qquad (5)$$

where each beam consists of B bunches with cross section A, N_{e^-} and N_{e^+} are the total number of particles in the electron and positron beams, respectively, and the revolution frequency of the beams in the storage ring is f_{rev}[1]. The luminosity of a storage ring provides a measure of its instantaneous performance, but high luminosity is of little use if significant time is lost filling or tuning the ring. To produce the most collisions for CLEO, the goal is to maximize the number of collisions achieved during each running period. Thus, time-integrated luminosity is a more useful measure of performance.

1. Dynamic Aperture

As the beams travel through the ring, their transverse size is clearly limited by the inner dimensions of the beam pipe. Particles on a trajectory that places them beyond this *physical aperture* will hit the pipe wall and be lost, thus reducing the current in the beam. The actual displacement from the design orbit that a particle can endure without being lost, however, is generally much smaller. This *dynamic aperture* is defined by the electromagnetic field in CESR, which includes both the fields intentionally produced by the lattice and unintentional contributions from BBI and imperfections in the guide magnets. Particles beyond the dynamic aperture experience forces—such horizontal defocusing from LRBBI, or nonlinear regions in the dipoles or quadrupoles—that quickly push them out of the beam pipe. Few particles in CESR precisely follow the design orbit, and the variation in trajectories increases as the particles interact with the complicated electromagnetic field present in CESR. Dynamic aperture thus effects beam lifetime by reducing the number of stable trajectories, causing the beam to degrade faster and increasing the amount of time lost to topping off the beams. To maximize time-integrated luminosity, therefore, the dynamic aperture should be as large as possible to reduce the rate of beam degradation.

2. Welch/Temnykh B Parameter

The Welch/Temnykh B parameter is a value related to LRBBI that has been experimentally determined to relate to lifetime. The B parameter of a lattice is given by

$$B = I_b \gamma \sqrt{\sum_{PCs} \left(\frac{\beta_y \sigma_x^2}{4\Delta x_{pc}^2}\right)^2}, \qquad (6)$$

the sum of the root mean square vertical kicks imparted to the beam at each parasitic crossing. It is proportional to the beta function[2] in y, the root mean square beam size in x, the horizontal separation between the beams at each parasitic crossing, the positron bunch current, and the energy of the beam. It has been experimentally determined that a smaller Welch/Temnykh B parameter corresponds to a longer lifetime, which makes physical sense: a smaller B parameter implies a smaller net vertical displacement and thus less divergence of the beam from the design orbit. Two straightforward ways to lower the B parameter are to reduce the bunch current, which would sacrifice luminosity, or to increase Δx_{pc} by increasing the pretzel amplitude.

3. Horizontal BBI Kicks

The beams also receive horizontal kicks from BBI, both from horizontal defocusing at the parasitic crossings and–if the beams are poorly collided–from LRBBI-like repulsion between the non-colliding regions of the beams at the IP. As with vertical kicks in the Welch/Temnykh B parameter, large horizontal kicks reduce beam lifetime by pushing particles away from the design orbit and further into the fringes (or beyond) of the dynamic aperture.

[2] See section I.C.4 of this paper.

4. Phase Space

Each particle in a beam can be described by the six coordinates $(x, p_x, y, p_y, \sigma, E)$, where σ is the longitudinal position of the particle relative to the bunch center. This six-dimensional space is called *phase space*. Assuming that the beam energy is approximately constant, the slopes x' and y' of the trajectories are proportional to the transverse momenta. Thus, at any given location in CESR the behavior of the beam can be characterized by its extent in x/x' and y/y' phase planes. By creating scatter plots of the locations of a beam's particles in the x/x' and y/y' phase space, a representative *phase ellipse* can be drawn about the phase space of the beam at each element in CESR. By Liouville's theorem (Wiedemann, 155), the area of this ellipse—also known as the *emittance*, ϵ, of the beam—remains constant under a given configuration of the CESR lattice when the beam's energy is assumed to be constant. Fig. 4 shows how the phase ellipse is transformed by a focusing quadrupole, which produces a *beam waist*—a minimum in the transverse beam size—at its focal point. The shape of the ellipse at

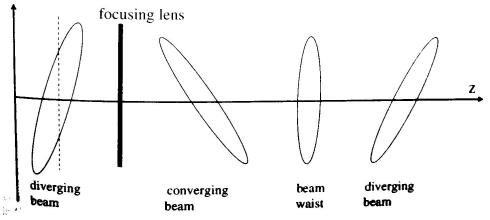

Figure 4: The transformation of a phase ellipse as it passes through a focusing quadrupole. [3]

each point z along the trajectory is given by

$$\gamma(z)x(z)^2 + 2\alpha(z)x(z)x'(z) + \beta(z)x'(z)^2 = \epsilon, \quad (7)$$

where α, β, and γ are known as the *Twiss parameters* of the beam[3]. Fig. 5 shows the relationship between the Twiss parameters and the phase ellipse at a given point in the trajectory. Note that $\sqrt{\beta}$ is proportional to the horizontal extent of the beam. Thus to improve luminosity a lattice should produce the lowest possible emittance and have a *beam waist*, indicated by a local minimum in β, at the IP.

D. Old and New CESR-c Lattices

In 2005, the lattice 12wig_20050626a was designed and implemented in CESR-c. 12wig produces high luminosity, but is incapable of injecting into collision. This caused significant time losses since the

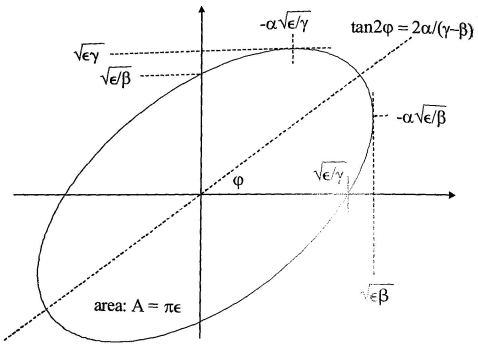

Figure 5: Phase ellipse with Twiss functions. [3]

beams had to be periodically dumped and refilled from scratch, resulting in reduced time-integrated luminosity. This was rectified by J. Hylas through extensive empirical tuning of the lattice, resulting in a new lattice configuration capable of both top-off injection and high luminosity. This modified lattice was used during the last CESR-c running period, and was reverse-engineered into a model called fit_postop_20070116.

For CESR-c's final physics run, a new lattice called 3770_inj_20070606_2p0 has been designed with the goal of further improving injection efficiency while maintaining or exceeding the time-integrated luminosity achieved by the modified 12_wig lattice. This lattice is unique in that it is optimized for small beam size at the IP at 2.0mA of positron bunch current, while all previous lattice designs have been optimized at 0mA positron bunch current. This is predicted to reduce the effects of BBI in this lattice, resulting in both easier injection and higher luminosity. To enhance the accuracy of the model, known multipole field errors were added to 3770_inj_20070606_2p0 to produce 3770_inj_20070606_2p0_mult. The behavior of 2p0_mult was not observed to differ significantly from that of 2p0, but the multipole terms are retained in the simulations to improve accuracy.

III. Modeling

The behavior of electrons in fit_postop and 2p0_mult was modeled using two Fortran90 programs, *bunch* and *dynap_scan*. *Bunch* calculates the effect of BBI on the design orbit for one idealized[3]

[3] *Bunch* assumes that each electron starts on the lattice's design orbit at the design energy.

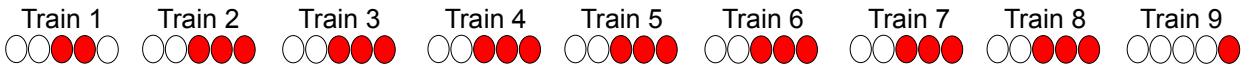

Figure 6: Positron bunch configuration from 3/7/06. Red and white ovals represent filled and empty positron bunches, respectively.

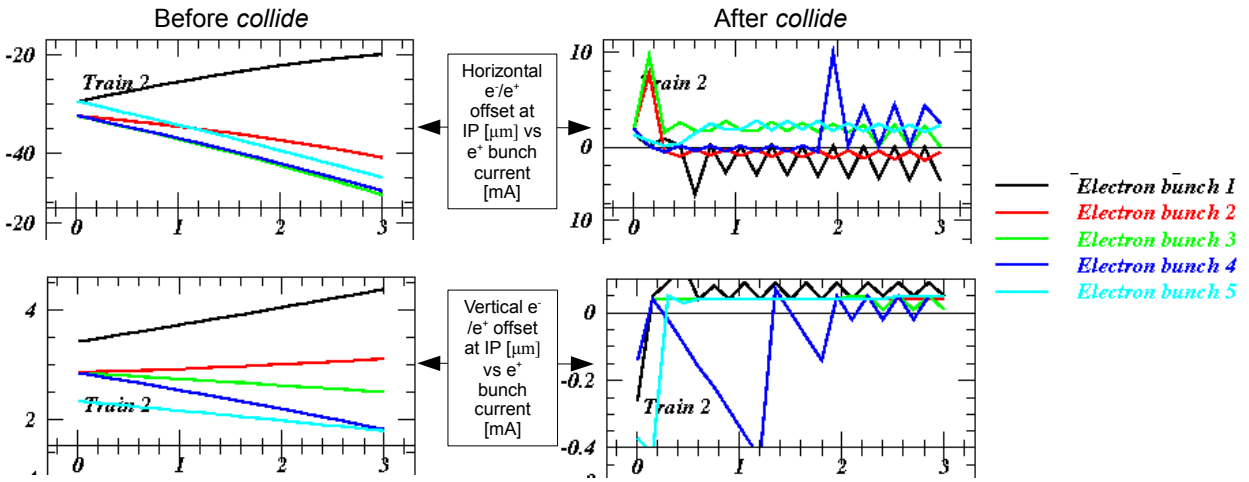

Figure 7: A comparison of the horizontal and vertical offsets between the beams at the IP before and after the implementation of the *collide* subroutine.

representative electron from each of 45 bunches, configured in 9 trains of 5 bunches. In addition to tracking the position and momentum of each bunch's representative electron, *bunch* also calculates the horizontal separation between the beams and the dynamic aperture at the IP, as well as the B parameter, Twiss functions, and a number of other parameters. This is done by drawing upon the BMAD libraries[7], Cornell's repository of Fortran90 subroutines for simulating relativistic charged-particle dynamics in storage rings and accelerators. *Bunch* also includes a multitude of user-defined parameters, including the lattice and the configuration of positron bunches. In this analysis, 3770_inj_20070606_2p0_mult was used with the modified 8x3 positron configuration shown in Fig. 6. This positron configuration was empirically determined to provide good performance during the last CESR-c running period with fit_postop, so it was adopted for this analysis to allow direct comparison between the fit_postop and 2p0_mult models. The program *dynap_scan*, developed by M. Van Camp, was created by modifying *bunch* to calculate dynamic aperture width at the IP while looping over positron bunch current and the parameter *prz1*, which alters the crossing angle of the beams at the IP by increasing the amplitude of the pretzel orbits. The data produced by *bunch* and *dynap_scan* were analyzed by programs written in Physics Analysis Workstation[8] by J. Crittenden and M. Van Camp.

IV. Results/Analysis

A. "Collide" Routine

Fig. 7 compares the horizontal and vertical e^-/e^+ offsets at the IP versus positron bunch current in 3770_inj_20070606_2p0_mult before and after implementing the *collide* routine. Without *collide*, at 3mA of positron bunch current (the operating current last used in CESR-c) the beams were offset about 50 microns horizontally and 3 microns vertically. Since the beams measure about 300 by 5 microns, this amounts to only 33 percent of the available beam cross section being in collision. After implementing *collide*, however, the horizontal and vertical offsets near 3mA reduced to 5 microns and 0.1 microns, respectively, resulting in 96 percent collision. Since we are concerned with accurately modeling high-energy physics conditions, *collide* is used throughout the remainder of this analysis.

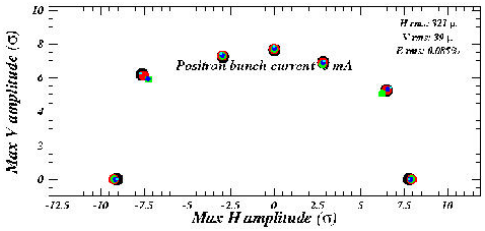

(a) 0.0 mA e+ bunch current, 0σ energy offset

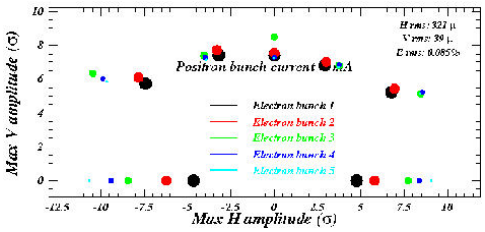

(b) 3.0 mA e+ bunch current, 0σ energy offset

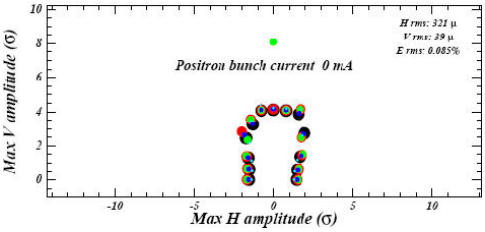

(c) 0.0 mA e+ bunch current, 3.5σ energy offset

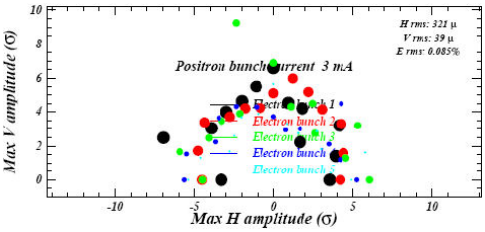

(d) 3.0 mA e+ bunch current, 3.5σ energy offset

Figure 8: Dynamic apertures for fit_postop

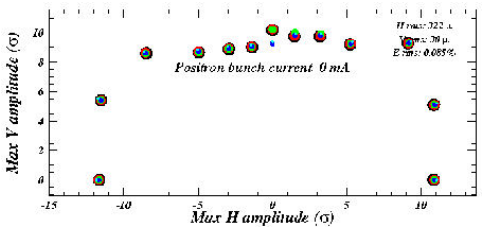

(a) 0.0 mA e+ bunch current, 0σ energy offset

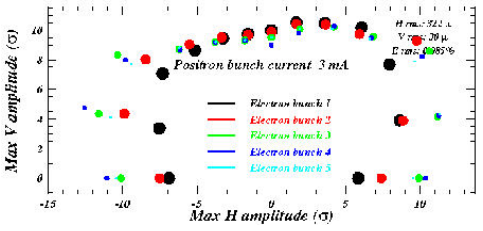

(b) 3.0 mA e+ bunch current, 0σ energy offset

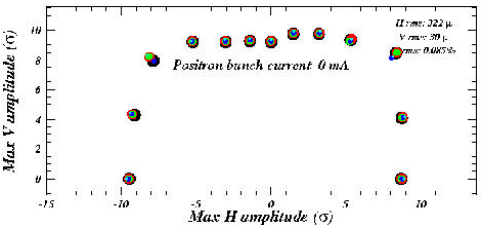

(c) 0.0 mA e+ bunch current, 3.5σ energy offset

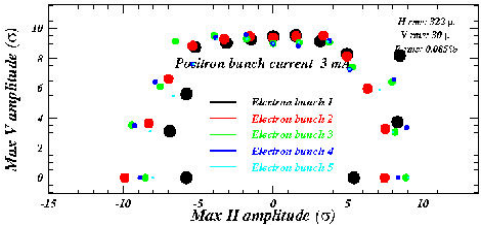

(d) 3.0 mA e+ bunch current, 3.5σ energy offset

Figure 9: Dynamic apertures for 2p0_mult

B. Dynamic Aperture

Using the last CESR-c running conditions, the fit_postop lattice was used to provide a baseline dynamic aperture that 2p0_mult must minimally achieve to be considered as a replacement for fit_postop. Fig. 8 shows the dynamic aperture in units of root mean square beam size for fit_postop for both on- and off-energy electrons, with and without positron current, using the default tunes and pretzel amplitudes found for the reverse-engineered lattice. Fig. 8 represents the baseline performance that 2p0_mult should meet–and hopefully exceed–to justify adopting it as a new lattice. The largest observed dynamic aperture is for on-energy electrons with no positron current, and is over twenty times the rms width of the beam (Fig. 8(a)). It makes sense that this combination performs best in fit_postop: since the particles are at the design energy, they are traveling along the central orbit and thus receiving the proper kicks from each element in the lattice, which was designed to operate at 0.0 mA positron current. Increasing the positron bunch current to 3.0 mA causes the dynamic aperture to change for each bunch as some experience IPBBI (bunches 3-5), and all experience LRBBI at a different point in their betatron oscillation (Fig. 8(b)).Off-energy bunches experience a

very small dynamic aperture (Fig. 8(a)), which is improved by beam-beam interaction (Fig. 8(d)). Of these four cases, the off-energy case with BBI is most representative of the conditions experienced by an average electron.

Dynamic apertures were calculated for 2p0_mult at 3.0 mA positron current, 3400 units of prz1, and with the tunes fixed at qx=0.518 and qy=0.590.[4] As seen in Fig. 9, 2p0_mult can clearly achieve larger dynamic apertures than fit_postop, both with and without BBI, and has a particularly robust dynamic aperture for off-energy bunches experiencing BBI (Fig. 9(d)). Since 2p0_mult is capable of producing larger dynamic apertures than fit_postop, the question naturally arises as to which combination of positron current and prz1 amplitude produces the largest dynamic aperture at or above the previous running currents. This combination would minimize the effect of dynamic aperture on lifetime, as well as improve luminosity by increasing the positron current. The search for this combination was accomplished by *dynap_scan*, which examined the effect of positron current and prz1 amplitude on the width of the dynamic aperture along the x-axis. Fig. 10 shows the dynamic aperture width in units of root mean square beam size at the interaction point versus the positron bunch current in milliamps and the prz1 amplitude for each bunch in train two [5]. This plot is for off-energy bunches, which are more relevant for lifetime. There is large dynamic aperture throughout this region, with a peak for colliding bunches near 3.6 mA positron current and 4000 units of prz1 amplitude.[6]

C. Testing dynap_scan

Dynap_scan suggests that this is the optimal combination of positron current and prz1 amplitude for maximizing dynamic aperture and thus increasing beam lifetime. It behooves us, however, to confirm that this combination is likely to actually give high time-integrated luminosity. This is does by comparing *dynap_scan*'s 'optimal' solution to the default settings for 2p0_mult through other parameters that effect time-integrated luminosity: the Welch/Temnykh B parameter, the BBI kicks throughout the ring, and the 500-turn phase space at the IP.

1. Welch/Temnykh B Parameter

At 3.6 mA positron bunch current, the average contribution to the Welch/Temnykh B parameter at each parasitic crossing is 0.042 for the design tunes and prz1 amplitude (Fig. 11(a)). The optimized parameters reduced the average contribution to 0.021 (Fig. 11(b)). This is a significant improvement, but it is not, however, the lowest possible B parameter for this lattice. Prz1 values from 3100 to 5000 were tested, with the lowest observed B parameter occurring at the highest prz1 amplitude (Fig. 11(c)). This makes physical sense; the B parameter is inversely proportional to Δx_{pc}, so by increasing the pretzel amplitude, the beams are pulled further apart at the parasitic crossings and their interaction is reduced. While the optimized parameters do not absolutely minimize the B parameter, they do significantly reduce it and should thus improve beam lifetime.

2. BBI Kicks

Under the design parameters, the BBI kicks throughout the ring ranged between ±0.01mrad at 3.6 mA positron bunch current. The ranged was reduced to ±0.005mrad under the optimized conditions, which can once again be explained by the increased beam separation caused by the higher prz1 amplitude. This can be seen in Fig. 12: the maximum horizontal separation between the beams increased from 2.5cm under the default settings to nearly 3.5cm under the optimized settings.

3. 500-Turn Phase Space at the IP

The 500-turn phase space at the IP was found at 3.6 mA positron current for the design parameters, the optimized parameters, and for a range of prz1 amplitudes at the tunes used in the optimized parameters (prz1=[3100-5000]). Negligible change was observed in the y/y' plane, but some variation was found in x/x' (Fig. 13). Interestingly, the smallest observed x/x' phase space occurred at the optimal parameters, suggesting that 4000 units of prz1 amplitude minimizes emittance at this current. The

[4] These tunes were chosen because injection efficiency and luminosity analysis on this lattice were being conducted by the accelerator group with this tune combination; they do not necessarily represent the optimal tunes for this lattice, but they were adopted to provide consistency between simulations. This analysis does not consider other tune combinations for this lattice.

[5] Note that in train 2 only bunches 3-5 are colliding.

[6] The higher peak near 1mA positron bunch current and 3200 units prz1 amplitude was rejected due to its low current, which would dramatically reduce luminosity.

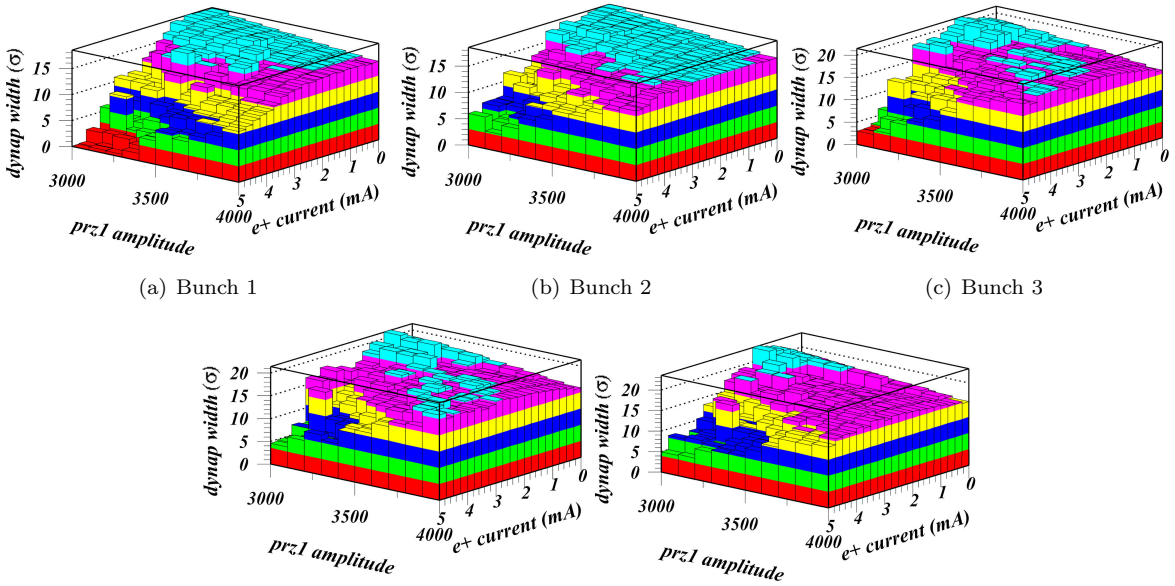

(a) Bunch 1 (b) Bunch 2 (c) Bunch 3

(d) Bunch 4 (e) Bunch 5

Figure 10: Dynamic aperture width in units of rms horizontal beam size versus e+ bunch current in mA and prz1 amplitude for bunches 1-5 of train 2.

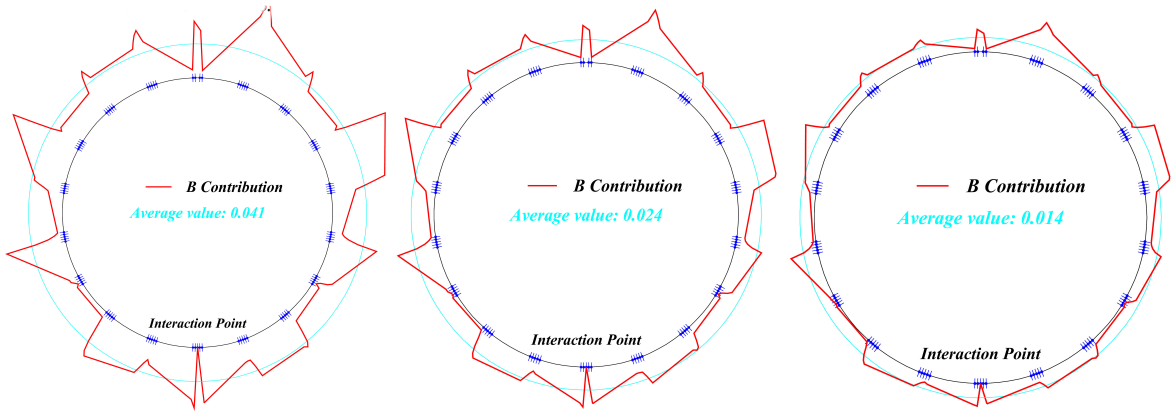

(a) Design parameters (b) Optimal parameters (c) prz1=5000, qx=.518, qy=.590

Figure 11: Welch/Temnykh B parameters for 2p0_mult at 3.6 mA e+ current

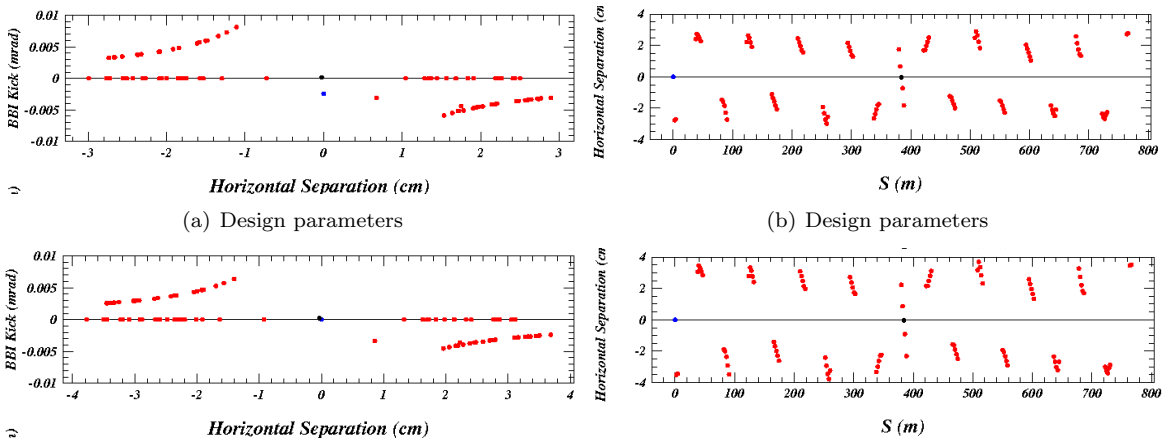

(a) Design parameters (b) Design parameters

(c) Optimal parameters (d) Optimal parameters

Figure 12: BBI kicks versus horizontal separation (12(a) and 12(c)) and horizontal separation versus position (12(b) and 12(d)) for 2p0_mult at 3.6 mA e+ current

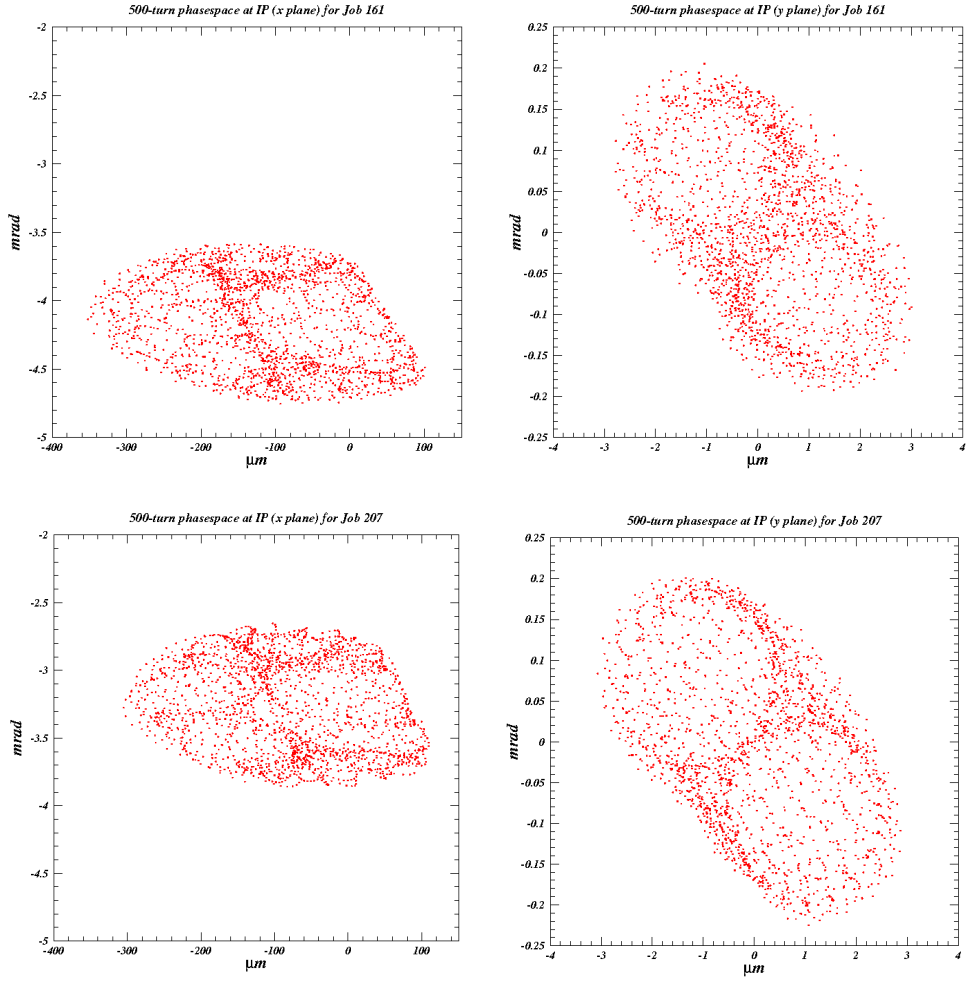

Figure 13: 500-turn phase space in the x/x' (left) and y/y' (right) phase planes for 2p0_mult under the default (top) and optimized (bottom) conditions.

reduction in the 500-turn x/x' phase space is, admittedly, fairly small, but the coincidence of maximum dynamic aperture and minimum phase space at these parameters supports the conclusion that the horizontally defocusing effects of LRBBI are minimized by this combination of current and pretzel amplitude.

V. Conclusion

The new lattice 2p0_mult is capable of providing larger dynamic apertures at the interaction point than were achieved—according to the reverse-engineered lattice fit_postop—during the previous running period. The program *dynap_scan* successfully optimized the dynamic aperture on the x-axis at the IP with respect to positron bunch current and prz1 amplitude. The optimal combination—3.6 mA positron bunch current and 4000 units of prz1 amplitude—was found to also roughly halve both the Welch/Temnykh B parameter and BBI kicks throughout the ring, and to minimize the 500-turn phase space at the IP. This suggests that *dynap_scan* is a useful tool for improving time-integrated luminosity, since the same bunch current and prz1 amplitude that maximize dynamic aperture at a given tune and positron bunch configuration also improve other lifetime and luminosity related parameters. This has practical applications for the implementation of 3770_inj_20070606_2p0 in CESR, as it may reduce the amount of tuning required to achieve the desired time-integrated luminosity. *Dynap_scan*, however, currently calculates dynamic aperture by assuming that every particle in the beam is launched parallel to the design orbit at the IP. This simplification may be providing overly optimistic estimates of the dynamic aperture, and should be resolved in future development of *dynap_scan* and the *dynamic_aperture* BMAD subroutine.

VI. Acknowledgments

Many thanks to Dr. Jim Crittenden, for his excellent advising and teaching. Thanks also to Mr. Mike Forster and Dr. Dave Rubin for their comments, criticism, and occasional collaboration. Thanks to Mr. Jim Shanks for his assistance in learning Fortran and navigating the BMAD libraries. Finally, thanks to Dr. Rich Galik, Ms. Peggy Steenrod, Ms. Monica Wesley, and the others at Cornell and the National Science Foundation who made the LEPP REU program possible. This work was supported by the National Science Foundation REU grant PHY-0552386 and research co-operative agreement PHY-0202078.

References

[1] D. Edwards and M. Syphers, *An Introduction to the Physics of High Energy Accelerators.* John Wiley & Sons: New York, 1993.

[2] E. D. Courant, M. S. Livingston, and H. S. Snyder, "The strong-focusing synchrotron—a new high energy accelerator," *Phys. Rev.*, vol. 88.

[3] H. Wiedemann, *Particle Accelerator Physics, 3rd Ed.* Springer: Berlin, 2007.

[4] M. Billing and J. Crittenden, "Beam-beam interaction studies at the cornell electron storage ring," *Phys. Rev. ST Accel. Beams*, vol. 9, 2006.

[5] M.G. Billing and J.A. Crittenden, Proceedings of the 2006 Particle Accelerator Conference, 26-30 June 2006, Edinburgh, Scotland.

[6] M.G. Billing, J.A. Crittenden and D.L. Rubin, Proceedings of the 2005 Particle Accelerator Conference, 16-20 May 2005, Knoxville, Tennessee.

[7] *BMAD Library.* https://accserv.lepp.cornell.edu/cgi-bin/view.cgi/trunk/src/.

[8] *Physics Analysis Workstation. http://paw.web.cern.ch/paw/.*